The flow interaction of air distribution with thermal plumes and the effect on the air velocity fluctuation under increased heat load conditions

Sami Lestinen[*1], Simo Kilpeläinen[1], Risto Kosonen[1], Juha Jokisalo[1], and Hannu Koskela[2]

1 Aalto University, School of Engineering
Sähkömiehentie 4
02150 Espoo, Finland
**Corresponding author: sami.lestinen@aalto.fi*
Presenting author: Sami Lestinen

2 Turku University of Applied Sciences
Lemminkäisenkatu 14-18 B
FI-20520 Turku, Finland

ABSTRACT

Flow interaction between thermal plumes and vertical air distribution and the resulting airflow structures were investigated under increasing heat load conditions. The main objective was to investigate the large-scale flow patterns, airflow fluctuation and frequency of the flow field. The flow interaction between thermal plumes and ventilation provides random flow motion and vortical structures that further effect the airflow characteristics such as velocity and temperature fields, turbulence intensity and frequency of the fluctuations. Fourier analysis was conducted in order to observe the energy levels of air speed records. It represents the frequency distribution from the set of discrete values of the given variable over the time-interval by providing the sinusoidal components of original function with certain frequency. The novelty of this study comes from the Fourier analysis of this flow interaction. The flow interaction was investigated in a test chamber of 5.5 m (l) x 3.8 m (w) x 3.2 m (h). Thermal plumes were produced by using 12 symmetrically installed cylindrical thermal loads of 0.4 m x 1.1 m that gave a thermal load range of 40-80 W/m^2-floor. Omnidirectional anemometers were installed into a measuring mast at the heights of 0.1 m, 0.6 m, 1.1 m, 1.7 m, 2.3 m and 2.9 m. The highest mean air speed was observed near the floor at the height of 0.1 m and the lowest near the top of thermal loads at the height of 1.1 m. The smallest turbulence intensity in turn was near the floor at the height of 0.1 m, whereas the highest intensity was found at the height of 1.1 m. The draught rate *DR* was below 21 %, and it increased with heat load. The highest draught rate was observed near the floor and the smallest at the height of 1.1 m, similarly than in the mean air speed and conversely than in the turbulence intensity. Overall, the results indicate a clear correlation between the thermal load level and the mean air speed as well as the airflow fluctuation. The observations showed that the mean air speed, the airflow fluctuation and the power spectral density increased with thermal load.

KEYWORDS

Thermal environment, buoyancy flows, convection flow, airflow structure, flow interaction, Fourier analysis

1 INTRODUCTION

Thermal comfort is a condition of mind that express satisfaction with thermal environment as represented in EN ISO Standard 7730:2005 (CEN, 2005) and in ASHRAE Standard 55 (ANSI/ASHRAE, 2013). This means that when a person feels thermally neutral or cooler, the increased local heat loss due to higher velocity may cause a local discomfort because of a sensation of draught. Furthermore, the risk of draught increases when the airflow temperature decreases and the mean velocity and the turbulence intensity increase. In an earlier study, Kovanen et al. (1987) found that the energy spectrum is proportional to the mean velocity such that the energy increases with mean velocity. Fanger et al. (1988) proposed that the

turbulence intensity has a significant effect on the sensation of draught. In a subsequent study, Melikov et al. (1997) showed that also temperature fluctuation increase draught sensation.

Indoor airflows are typically turbulent. The mean air speed can be usually 0.05-0.6 m/s with the turbulence intensity of 10-70 % and the significant level of fluctuations are mainly up to 1 Hz frequency with variable air speed, fluctuation and flow direction (Melikov et al., 2007). The turbulent flow is unsteady and random flow motion that is related to a wide range of length and time scales (Tennekes and Lumley, 1972; Etheridge & Sandberg, 1996; Pope, 2000). Turbulent kinetic energy is produced from the mean flow into the largest eddies and the energy is then further transferred to the smaller and still smaller eddies until it is dissipated to the heat mainly from the smallest eddies. The turbulence increases the flow disturbances and the interaction between the vorticity and the velocity gradients in the flow. Turbulence also improves the transform of energy but requires continuous supply of energy against the turbulent stresses (Townsend, 1976).

Also the airflow interaction has an effect on flow structures. The physics of flow interaction may come from the advection, viscous and buoyancy forces, together with static pressure differences and turbulence production, which provide random, transient and vortical flow motion, that can further yield a draught discomfort in an occupied zone. The low-frequency fluctuation can then be closely related to the convection, thus advection and viscous forces. Nielsen (2011) represented that depending on *Ar*-number, which describes the ratio between the buoyancy and the inertial forces, the airflows can be classified into the momentum driven or the buoyancy driven flows. The earlier studies also indicate that a plume flow is continuously fluctuating (Kofoed & Nielsen, 1988). In a subsequent study, Kosonen et al. (2010) showed that velocity field is greatly affected by the strength of a heat source and its distribution in a room. Furthermore, Zukowska et al. (2012) emphasized that thermal plumes from low-heat sources are very sensitive to the surroundings and the source itself. In addition, Kandzia (2013) studied a transient flow behavior of detailed flow structures under natural and forced convection, and Müller et al. (2013) demonstrated a significance of flow interaction in an indoor environment. Noteworthy is also that the natural convection flows seem to dominate in the highly occupied enclosures, and the buoyancy-driven convection flows may have a higher effect on the flow field than the previous studies have indicated (Kosonen et al., 2016). In any case, the air distribution can be difficult to control in an occupied zone (Melikov, 2016).

Previous studies have indicated that draught is one of the most challenging thermal comfort problem in buildings with high or moderate level of cooling loads. In practice, the complex interaction of jets and thermal plumes makes the analysis of the air distribution and further the local thermal comfort difficult. It should also be noted that the local thermal comfort index of the draught rate (*DR*) is not able to take into account of turbulent frequency and scales. In this study, the main objective is to analyse the air speed fluctuation and turbulence scales with increasing heat load levels in the case that the low-momentum supply airflow rate is released through a diffused ceiling and when the internal heat loads are installed symmetrically in the occupied zone. The novelty of this study comes from detailed information of airflow fluctuation under high thermal load levels between the thermal plumes and vertical air distribution in a varied thermal environment.

2 METHODS

2.1 Test chamber

The measurements were carried out in a test chamber of 5.5 m (L) x 3.8 m (W) x 3.2 m (H) (Figure 1). The vertical air distribution was introduced by discharging supply air through a diffused ceiling into the occupied zone. The suspended ceiling was 0.35 m below the ceiling envelope. The suspended ceiling was made of perforated glass-wool-plate elements with the open perforation area of 0.5%. The diameter of drilled holes was 14 mm. The duct-diffuser combination with diameter of 0.2 m extended the entire length of upper chamber and produced rather equal supply air distribution, in which the static pressure difference forces the airflow through the suspended ceiling down to the occupied zone.

2.2 Experimental set-up

The experimental set-up was conducted by using 12 cylindrical test dummies (Figure 1). The diameter of the heat source was 0.4 m (Zukowska et al., 2012), and the height of the dummy was 1.1 m (Standard EN 14240:2004). The heat sources were placed evenly on the floor (Figure 2). The thermal load was increased gradually such that specific heat load was 40-80 W/m^2-floor as shown in Table 1. The effect of supply air temperature was investigated by keeping the target temperature at 26°C in the reference location 9 at the height of 1.1 m (Figure 2). The dummy temperature differences were observed by conducting an infrared camera. The flow field was measured using 6 hot-sphere anemometers and visualised with smoke and low-weight ribbons attached to the suspended ceiling. The anemometers were installed into a measuring mast at the height of 0.1 m, 0.6 m, 1.1 m, 1.7 m, 2.3 m and 2.9 m (EN ISO 7726:2001). The three lowest sensors were the Vivo Draught 20T31 omnidirectional anemometers and the three highest sensors were the Sensoanemo 5100SF omnidirectional anemometers. The readings were between 1 s and 2 s, respectively. Hence, the Vivo Draught anemometers reach the 1 Hz frequency at the region between 0.1 m and 1.1 m. The symmetrical set-up offered a smaller investigation region in which the different locations can be classified as follows. The first group was the locations between the cylindrical thermal loads in a longitudinal direction (L), i.e. locations 3, 4, 7, 9. The second group was the locations between four thermal loads, i.e. locations 2, 8, 10. The third group was the locations between two thermal loads in a wide-wise direction (W), i.e. locations 1 and 5. In addition, one location was 20 cm from the wall at the location 6.

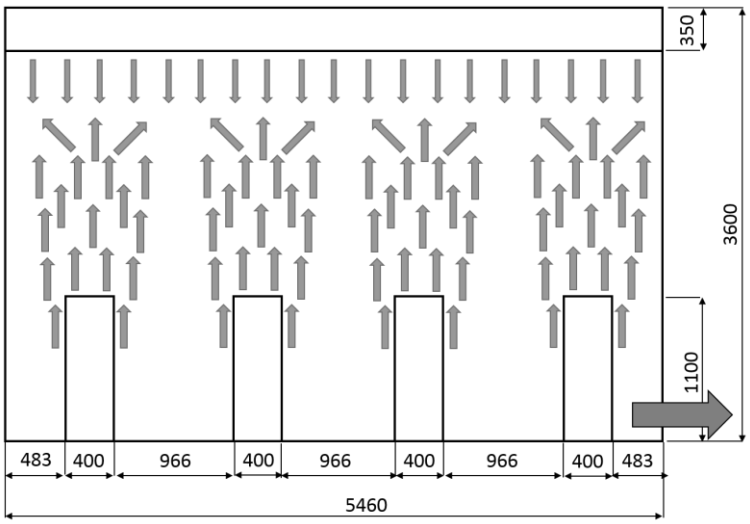

Figure 1: A schematic flow chart (mm) regarding with thermal plumes and vertical air distribution in a simplified thermal environment. The exhaust valve was at the height of 0.4 m (arrow at the right side wall).

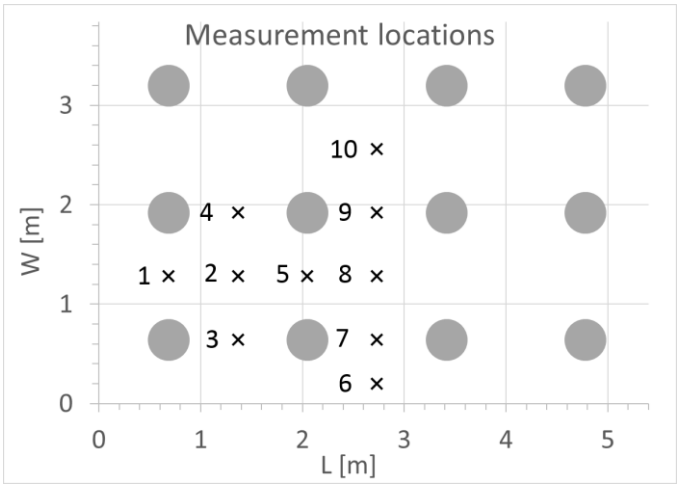

Figure 2: The measurement locations 1-10 and the cylindrical heat sources.

Table 1: The test cases

Test cases	Case 1	Case 2	Case 3	Case 4	Case 5	Case 6	Case 7	Case 8	Case 9
Heat load [W/m^2]	40	57	80	40	57	80	40	57	80
Supply air [l/s,m^2]	3.6	5.2	7.3	2.8	4.2	6.0	4.6	6.8	9.6
Supply air temp [°C]	17	17	17	15	15	15	19	19	19
Target temperature	26	26	26	26	26	26	26	26	26

2.3 Characterising the flow field

The Reynolds number and the Archimedes number describe the flow conditions and relationships of different forces accelerating the flow. The airflow fluctuation in turn can be investigated by dividing the given variable in a time-averaged component and in a fluctuating component as

$$\phi(x_i, t) = \bar{\phi}(x_i) + \phi'(x_i, t) \tag{1}$$

where ϕ is the variable, x refers to coordinate system, t is the time, $\bar{\phi}$ is the time-averaged component and ϕ' is the fluctuating component, and subscript i denotes the index notation. The time-averaged component is expressed as

$$\overline{\phi}(x_i) = \lim_{T\to\infty} \frac{1}{T} \int_0^T \phi(x_i, t)\, dt \tag{2}$$

where T is the averaging interval that should be sufficiently large compared to the fluctuating time-scale. Furthermore, the averaging discrete set of records with certain interval N in a given location x_i can be expressed by the ensemble average as

$$\overline{\phi}(x_i, \mathrm{t}) = \lim_{N\to\infty} \frac{1}{N} \sum_{n=1}^{N} \phi(x_i, t) \tag{3}$$

where $\overline{\phi}(x_i, t)$ is the ensemble-averaged component dependent on both the location and time, and N is the number of discrete values in the interval that filter more rapid fluctuations. Consequently, the ensemble-averaged component $\overline{\phi}(x_i, t)$ at Eq. (3) is a sort of moving average of a certain time-interval at the location x_i, whereas the time-averaged component

$\overline{\phi}(x_i)$ at Eq. (2) is a mean value of a given time-interval at the location x_i. The deviation of sample can then be calculated by expressing the sample standard deviation as

$$\phi_{\mathrm{SD}} = \sqrt{\frac{\sum_N \left(\phi_N - \bar{\phi}\right)^2}{N-1}} \tag{4}$$

where *N* denotes the number of records in a data series. The turbulence intensity can then be defined as

$$Tu = \frac{u_{SD}}{\bar{u}} x100 \tag{5}$$

where u_{SD} is the standard deviation of air speed records and $\bar{u}$ is the mean air speed at the same location. The draught rate index in turn can be expressed as

$$DR = \left(34 - t_{a,l}\right)\left(\bar{u}_{a,l} - 0.05\right)^{0.62}\left(0.37 \cdot \bar{u}_{a,l} \cdot Tu + 3.14\right) \tag{6}$$

where $t_{a,l}$ is the local air temperature [°C], $\bar{u}_{a,l}$ is the local mean air velocity [m/s] and Tu is the turbulence intensity [%]. The Fourier transform of airflow fluctuation represents a frequency distribution from the set of discrete values of a given variable over the time-interval by providing the sinusoidal components of original function with certain frequency (Cochran et al., 1967; Welch, 1967). The Fourier transform can be expressed as

$$\hat{\phi}(\omega) = \int_{-\infty}^{\infty} \phi(t) e^{-i\omega t}\, dt \tag{7}$$

where ω is the angular frequency and *t* is the time. The angular frequency can be determined as $\omega = 2\pi f$ and $f = 1/t$ where *f* is the frequency. The outcome of the Fourier transform is the complex-valued function $\hat{\phi}(\omega)$. The frequency distribution can then be shown in real number set by taking the absolute value $\left|\hat{\phi}(\omega)\right|$ from the transformed function, which shows the magnitude spectrum. Furthermore, the power spectrum is determined by $\left|\hat{\phi}(\omega)\right|^2$. It follows after algebra that the discrete Fourier transform can be defined as

$$\hat{\phi}(f)_k = \sum_{j=1}^{N} \phi(t)_j e^{(-2\pi i(j-1)(k-1)/N)} \tag{8}$$

where *j* and *k* denotes the indexes and *N* is the sample of the discrete data set e.g. the given discrete time-interval set $T{=}N\Delta t$. The power spectral density describes the distribution of power as a function of frequency that provides the normalized power spectrum. The power spectral density is determined as

$$S(\omega) = \frac{1}{N}\left|\hat{\phi}(\omega)\right|^2 \tag{9}$$

where the divisor *N* normalize the result.

3 RESULTS

Thermal load levels in the measurements were produced with several combinations of supply air temperature and supply airflow rates. The given range of supply air temperature provided only 3% deviation on the mean air speed and below 1% on the standard deviation. This small

effect is an outcome from the low-momentum and vertical supply airflow. This means that the effect of air distribution through the diffused ceiling is not significant, and the buoyancy driven convection flows dominated the air distribution in the test conditions. Therefore, the following results include only one combination of supply air temperature and flow rate for each thermal load level (Cases 1-3).

3.1 Mean air speed

In the cases 1-3, the mean air speed over the measured locations was generally around 0.15 m/s with the mean standard deviation of 0.045 m/s and with the range of 0.08-0.25 m/s in the region below 1.1 m. At this region, the mean air speed over the measured locations increased around 47 % between the 40 W/m^2 and the 80 W/m^2. In this case, the range was slightly increased indicating more deviation in the flow field. On the contrary, the mean air speed was reduced about 40 % between the heights of 0.1 m and 1.1 m. The range was slightly decreased towards the top of the heat sources at 1.1 m, i.e. towards the lower air speed levels. Figure 3 shows the mean air speed against the room height at the given locations. Local differences exist but generally, the function characteristics are rather similar such that the mean air speed decrease from 0.1 m up to 1.1 m and increase with thermal load.

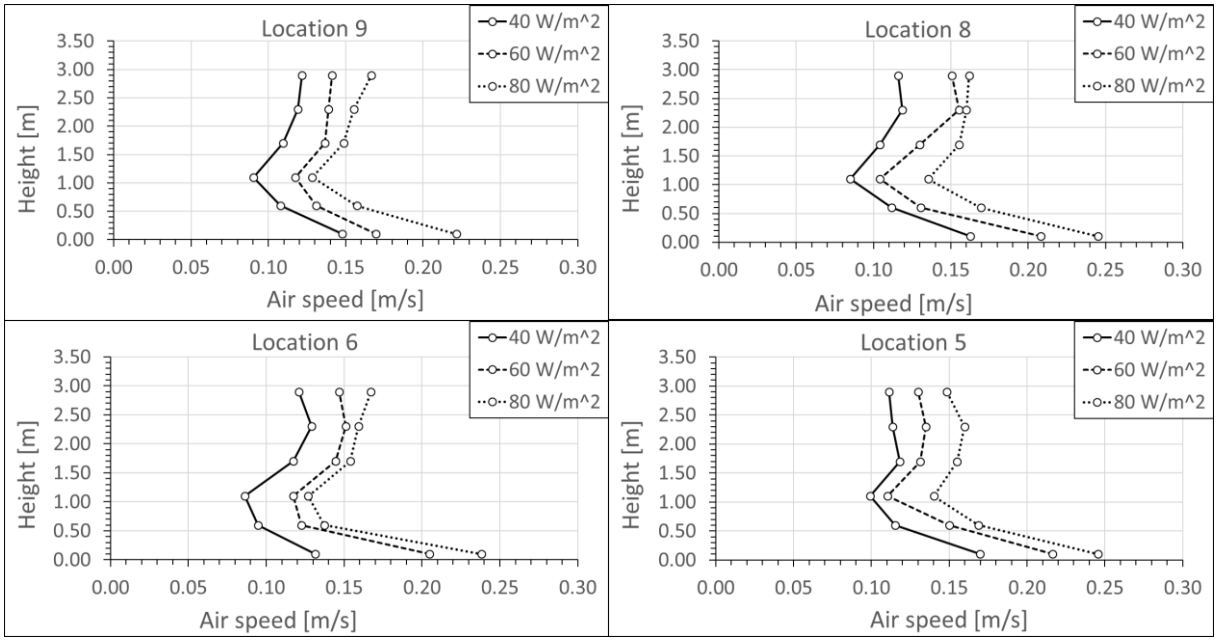

Figure 3: The mean air speed at the locations 5, 6, 8, 9 with the heat loads of 40 – 80 W/m^2, supply air 17°C, room target temperature below 26°C.

3.2 Airflow fluctuation

Figure 4 shows the mean air speed and the standard deviation at the height of 1.1 m in the location 8. The ensemble-averaged function over 60 s interval represents the filtered sinusoidal deviation of the data without faster fluctuation. The slow fluctuation may have a periodical deviation that occur as sinusoidal behaviour while proceeding the time axis further. The mean air speed was 0.085 m/s with the standard deviation of 0.051 m/s under the lowest thermal load of 40 W/m^2. The mean air speed increased 60 % up to 0.135 m/s towards the highest thermal load 80 W/m^2. The corresponding standard deviation increased 50 % up to 0.076 m/s, respectively. The increase of standard deviation describes the growing fluctuation that may have a significant effect on the sense of draught and

thermal comfort by increasing the heat transfer between the human subject and surroundings. The ensemble-averaged functions seem to have a certain periodicity between the local extrema and the additional information can be produced by conducting the Fourier analysis.

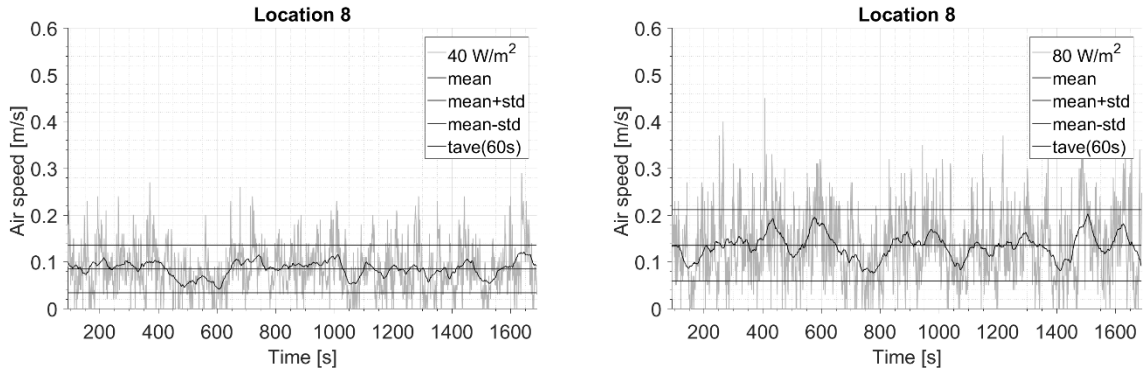

Figure 4: The air speed fluctuation, the mean air speed, the standard deviation and the ensemble time-averaged air speed over 60 s interval with the thermal loads of 40 W/m^2 and 80 W/m^2. Location 8 at the height of 1.1 m, case 1-3.

The turbulence intensity was rather constant regardless of the thermal load level. It seems that the mean velocity level had a bigger effect on the turbulence intensity than the prevailing thermal load level. Consequently, the smallest turbulence intensity was around 40 % near the floor at the height of 0.1 m, and the greatest intensity was about 60 % near the top of the thermal loads at the height of 1.1 m. This is mainly because the turbulence intensity increases towards the smaller mean velocity. The draught rate *DR* was below 21 % in the measured locations, and it increased with heat load. Furthermore, the highest draught rate was observed near the floor and the smallest at the height of 1.1 m. It seems that the European Standard EN ISO 7730:2005 (CEN, 2005) classifies this thermal environment mainly into the category B (*DR* 10-20 %) with the prevailing mean air speed, the air temperature and the turbulence intensity conditions.

3.3 Power spectral density

The mean power spectral density over the measured locations was about 3.9E−3 m^2/s^2 with the standard deviation of 9E−4 m^2/s^2 under the thermal load level of 40 W/m^2 in the considered region below the height of 1.1 m. The corresponding energy level with 80 W/m^2 was 6.8E−3 m^2/s^2 with the standard deviation of 1.4E−3 m^2/s^2. Consequently, the mean energy level was 74 % greater with 80 W/m^2 than with 40 W/m^2. This means that the fluctuation generally increased with thermal load. In addition, the standard deviation between the measured locations increased 54 %, which indicates also higher fluctuation in the flow field. The corresponding mean power spectral density was about 6.1E−3 m^2/s^2 with the standard deviation of 1.4E−3 m^2/s^2 at the height of 0.1 m and 4.5E−3 m^2/s^2 with the standard deviation of 1.4E−3 m^2/s^2 at the height of 1.1 m. Consequently, the mean power spectral density decreased 27 % up to the height of 1.1 m. Hence, it seems that the mean power spectral density decreases towards lower mean air speed levels. The standard deviation was almost the same level at both heights. Furthermore, the mean power was non-linearly dependent on the thermal load level and any specific frequencies were not recognized in the power spectral density function. However, the ensemble-averaged functions were higher with higher thermal loads (Figure 5, left). This means that the fluctuation energy was greater. However, the normalized function (Etheridge & Sandberg, 1996), that is the ratio of the power spectral density over the variance, was at the same level with varying thermal loads

(Figure 5, right). In contrast, this also indicates increasing fluctuation with thermal load due to change in variation. Furthermore, the power spectral density decreased relatively gradually towards increasing frequency. The significant energy differences were recognized in the neighboring frequencies and their multiplications while proceeding the frequency axis. The results are summarised in Table 2 and Table 3 where the mean air speeds and power spectral densities are shown with three heat loads levels and at different heights.

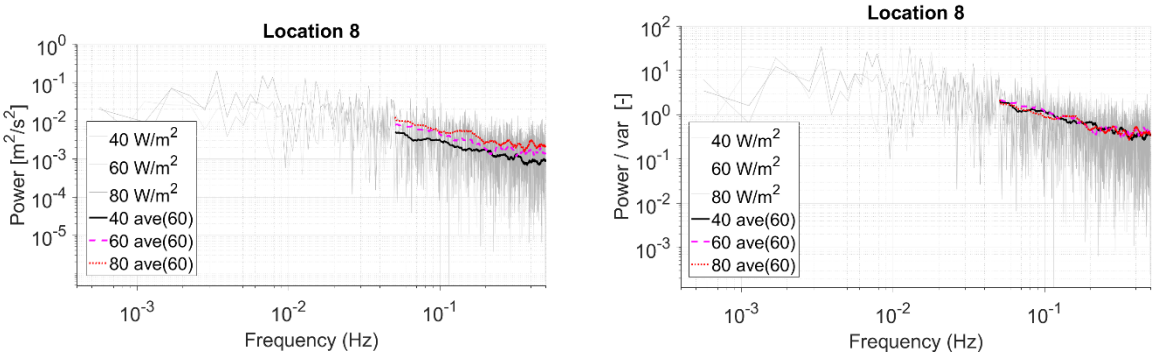

Figure 5: Airflow fluctuation with the different thermal loads: The power spectral density on the left and the normalised function on the right, log-log scales, at height 1.1 m, case 1-3.

Table 2: The statistics of the mean air speed of horizontal plane including locations 1-10 at the certain room height, reading interval 1 s, Cases 1-3.

Mean air speed	**0.1 m**	**0.6 m**	**1.1 m**	**0.1 m**	**0.6 m**	**1.1 m**	**0.1 m**	**0.6 m**	**1.1 m**
Heat load [W/m^2]	40	40	40	57	57	57	80	80	80
average	0.16	0.11	0.09	0.20	0.14	0.12	0.23	0.16	0.14
min	0.13	0.09	0.08	0.17	0.12	0.10	0.20	0.13	0.12
max	0.18	0.12	0.11	0.22	0.16	0.16	0.25	0.18	0.18
std	0.017	0.008	0.010	0.020	0.014	0.017	0.015	0.015	0.019
std/range	0.33	0.31	0.36	0.36	0.32	0.30	0.31	0.32	0.32

Table 3: The statistics of the mean power spectral density of horizontal plane including locations 1-10 at the certain room height, reading interval 1 s, Cases 1-3.

Power spectral density	**0.1 m**	**0.6 m**	**1.1 m**	**0.1 m**	**0.6 m**	**1.1 m**	**0.1 m**	**0.6 m**	**1.1 m**
Heat load	40	40	40	57	57	57	80	80	80
average	4.7E-03	3.8E-03	3.2E-03	6.0E-03	5.3E-03	4.5E-03	7.6E-03	6.9E-03	5.7E-03
min	3.7E-03	3.2E-03	2.6E-03	5.4E-03	3.9E-03	3.4E-03	5.9E-03	5.0E-03	4.3E-03
max	5.8E-03	5.1E-03	4.6E-03	6.9E-03	7.6E-03	6.7E-03	1.0E-02	9.1E-03	8.4E-03
std	6.8E-04	6.0E-04	6.8E-04	5.3E-04	1.0E-03	9.3E-04	1.1E-03	1.0E-03	1.3E-03
std/range	3.3E-01	3.2E-01	3.3E-01	3.5E-01	2.7E-01	2.8E-01	2.7E-01	2.5E-01	3.3E-01

4 CONCLUSIONS

The mean air speed, the standard deviation and the maximum air speed mainly increased with thermal load. Consequently, also the power of discrete Fourier transform increased. Furthermore, the mean air speed increased 47% from the thermal load level of 40 W/m^2 up to 80 W/m^2, and reduced 40 % from the height of 0.1 m up to 1.1 m. The mean turbulence intensity was at the same level regardless of the thermal load level. The smallest turbulence intensity was around 40 % at the height of 0.1 m and the greatest intensity was about 57 % at the height of 1.1 m. Therefore, it seems that the current mean air speed level had a greater effect on the turbulence intensity than the prevailing thermal load level. The draught rate (*DR*) was

generally below 21 %. The mean power spectral density increased 74 % from the thermal load level of 40 W/m^2 up to 80 W/m^2. This means that the air speed fluctuation increased towards higher thermal load level. In contrast, the mean power spectral density decreased 27 % from the height of 0.1 m up to 1.1 m in which the mean air speed was lowest. This in turn indicates that the air speed fluctuation decrease with mean air speed. However, the turbulence intensity usually increase towards decreasing mean air speed, thus the significance of fluctuation can be greater in the low velocity regions. Overall, both the mean air speed and the airflow fluctuation increased with thermal load mainly because the internal energy increased locally in the test chamber.

5 ACKNOWLEDGEMENTS

The authors wish to acknowledge L.V.Y. foundation, K. V. Lindholms foundation, Finnish Foundation for Technology Promotion (TES) and Sisäilmayhdistys ry (SIY/FiSIAQ) for financial support.

6 REFERENCES

ANSI/ASHRAE (2013). Standard 55-2013 – Thermal Environmental Conditions for Human Occupancy. Ashrae Inc, Atlanta, USA, ISSN 1041-2336.

CEN (2001). European Standard EN ISO 7726:2001, Ergonomics of the thermal environment. Instruments for measuring physical quantities (ISO 7726:1998).

CEN (2005). European Standard EN ISO 7730:2005, Ergonomics of the thermal environment — Analytical determination and interpretation of thermal comfort using calculation of the PMV and PPD indices and local thermal comfort criteria. European Standard EN ISO 7730:2005(E), 3rd edition, 2005-11-15, Geneva, Switzerland.

Cochran, W. T., Cooley, J. W., Favin, D. L., Helms, H. D., Kaenel, R. A., Lang, W. W., ... & Welch, P. D. (1967). What is the fast Fourier transform?. Proceedings of the IEEE, 55(10), 1664-1674.

Etheridge, D., & Sandberg, M. (1996). Building ventilation: theory and measurement. Chichester, UK, John Wiley & Sons, ISBN 0-471-96087-X.

Kandzia, C. (2013). Experimentelle Untersuchung der Strömungsstrukturen in einer Mischlüftung. E. ON Energy Research Center, RWTH Aachen University.

Kofoed, P., & Nielsen, P. V. (1988). Thermal Plumes in Ventilated Rooms: an experimental research work. Dept. of Building Technology and Structural Engineering, Aalborg University.

Kosonen R, Lastovets N, Mustakallio P, Carrilho da Graça G, Mateus NM, Rosenqvist M. (2016). The effect of typical buoyant flow elements and heat load combinations on room air temperature profile with displacement ventilation, Building and Environment, doi: 10.1016/j.buildenv.2016.08.037.

Kosonen, R., Saarinen, P., Koskela, H., & Hole, A. (2010). Impact of heat load location and strength on air flow pattern with a passive chilled beam system. Energy and Buildings, 42(1), 34-42.

Kovanen, K., Majanen, A., & Sirén, K. (1987). Huoneilman virtausnopeuden, nopeuden vaihtelutaajuuden ja turbulenssiasteen kartoitustutkimus. Teknillinen Korkeakoulu, LVI-tekniikan laboratorio, Raportti B17, Espoo, Finland (In Finnish).

Melikov, A. K. (2016). Advanced air distribution: Improving health and comfort while reducing energy use. Indoor air, 26(1), 112-124.

Melikov, A.K., Hanzawa, H., Fanger, P.O., 1988, Airflow characteristics in the occupied zone of heated spaces without mechanical ventilation. ASHRAE Transactions, Vol. 94, Part 1, pp.52-70.

Melikov, A. K., Krüger, U., Zhou, G., Madsen, T. L., & Langkilde, G. (1997). Air temperature fluctuations in rooms. Building and Environment, 32(2), 101-114.

Melikov, A. K., Popiolek, Z., Silva, M. C. G., Care, I., & Sefker, T. (2007). Accuracy limitations for low-velocity measurements and draft assessment in rooms. HVAC&R Research, 13(6), 971-986.)

Müller, D., Kandzia, C., Kosonen, R., Melikov, A. K., & Nielsen, P. V. (2013). Mixing Ventilation. Guide on mixing air distribution design. Federation of European Heating and Air-Conditioning Associations, REHVA, ISBN 978-2-930521-11-4.

Nielsen, P. V. (2011). The" Family Tree" of Air Distribution Systems. In Roomvent 2011. TAPIR Akademisk Forlag. ISBN 978-82-519-2812-0.

Pope S. B. (2000). Turbulent flows, Cornell University, Cambridge University Press, ISBN 0-521-59886-9.

Tennekes H. and Lumley J. L. (1972). A First Course in Turbulence, The MIT Press, ISBN 0 262 20019 8.

Townsend A. A. (1976). The Structure of Turbulent Shear Flow, 2nd edition, Cambridge University Press, ISBN 0 521 29819 9.

Welch, P. (1967). The use of fast Fourier transform for the estimation of power spectra: a method based on time averaging over short, modified periodograms. IEEE Transactions on audio and electroacoustics, 15(2), 70-73.

Zukowska, D., Melikov, A., & Popiolek, Z. (2012). Impact of personal factors and furniture arrangement on the thermal plume above a sitting occupant. Building and Environment, 49, 104-116.